



HAL
open science

Mirage: 2D Source Localization Using Microphone Pair Augmentation with Echoes

Diego Di Carlo, Antoine Deleforge, Nancy Bertin

► **To cite this version:**

Diego Di Carlo, Antoine Deleforge, Nancy Bertin. Mirage: 2D Source Localization Using Microphone Pair Augmentation with Echoes. ICASSP 2019 - IEEE International Conference on Acoustic, Speech Signal Processing, May 2019, Brighton, United Kingdom. pp.775-779, 10.1109/ICASSP.2019.8683534 . hal-02160940

HAL Id: hal-02160940

<https://hal.science/hal-02160940>

Submitted on 20 Jun 2019

HAL is a multi-disciplinary open access archive for the deposit and dissemination of scientific research documents, whether they are published or not. The documents may come from teaching and research institutions in France or abroad, or from public or private research centers.

L'archive ouverte pluridisciplinaire **HAL**, est destinée au dépôt et à la diffusion de documents scientifiques de niveau recherche, publiés ou non, émanant des établissements d'enseignement et de recherche français ou étrangers, des laboratoires publics ou privés.

MIRAGE: 2D SOURCE LOCALIZATION USING MICROPHONE PAIR AUGMENTATION WITH ECHOES

Diego Di Carlo[†], Antoine Deleforge[‡], and Nancy Bertin[†]

[†] Univ Rennes, Inria, CNRS, IRISA, France

[‡] Université de Lorraine, CNRS, Inria, LORIA, F-54000 Nancy, France

ABSTRACT

It is commonly observed that acoustic echoes hurt performance of sound source localization (SSL) methods. We introduce the concept of microphone array augmentation with echoes (MIRAGE) and show how estimation of early-echo characteristics can in fact benefit SSL. We propose a learning-based scheme for echo estimation combined with a physics-based scheme for echo aggregation. In a simple scenario involving 2 microphones close to a reflective surface and one source, we show using simulated data that the proposed approach performs similarly to a correlation-based method in azimuth estimation while retrieving elevation as well from 2 microphones only, an impossible task in anechoic settings.

Index Terms— Sound Source Localization, Image Microphones, TDOA Estimation, Supervised Learning.

1. INTRODUCTION

Sound source localization (SSL) consists in determining the position of a sound source from microphone signals in 3D space. In polar coordinates, most existing methods focus on estimating the directional of arrival, namely, azimuth and elevation angles. Though this task is performed routinely by humans, it still challenges today’s computational methods, in particular in the presence of reverberation or interfering sources (see [1] and [2] for a review). Computational approaches consist in two components. First, extracting features from audio data that are as independent as possible from the source’s content while preserving spatial information. Second, mapping these features to the source position. Two lines of research have been investigated to obtain such mappings: physics-based and learning-based approaches.

Physics-based approaches rely on a simplified sound propagation model [1, 3, 4, 5]. The free-field model is by far the most widely used one and assumes a single direct sound path from the source to each microphone. When the source is placed far enough, this yields a closed-form mapping from the sound’s time-difference-of-arrival (TDOA) in a microphone pair and the source’s azimuth angle in this pair. If multiple

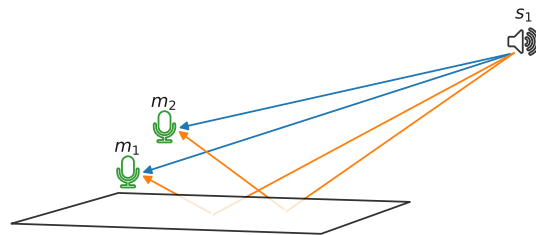


Fig. 1: Typical setup with one source recorded by two microphones. The illustration shows direct sound path (blue lines) and resulting first-order echoes (orange lines).

microphone pairs are available and form a non-linear array, their TDOAs can be aggregated to obtain 2D directions of arrival [4]. These methods strongly suffer in environments where the free-field assumption is violated, *e.g.*, in the presence of strong acoustic echoes and reverberation [6].

Learning-based approaches use an annotated training dataset to implicitly learn a mapping from audio features to source positions [7, 8, 9, 10, 11]. Such data can be obtained from real recordings [7] or using physics-based simulators [8, 9, 10, 11]. These methods were showed to overcome some limitations of the free-field model, but are usually trained for specific microphone arrays and fail whenever test conditions strongly mismatch training conditions.

Most sound source localization methods, including the above listed, regard reverberation and in particular acoustic echoes as a nuisance. In contrast, some recent work that we refer to as *echo-aware* methods have showed that the knowledge of early acoustic echoes could be used to reconstruct the geometry of an audio scene [12, 13, 14] or to improve performance of signal enhancement methods [15, 16, 17]. In [12], some ad-hoc reflectors are used as artificial *pinnae* to estimate elevation based on a simple reflection model. In [14], cameras, depth sensors and laser sensors are used to identify reflectors and build a corresponding acoustic model that helps SSL.

In this work, we combine ideas from physics-based, learning-based and echo-aware approaches to introduce the framework of microphone array augmentation with echoes (MIRAGE) for SSL. We consider a simple yet common scenario to illustrate this idea: two microphones, one source and

The research presented in this paper is reproducible. Code and data are available at <https://github.com/Chutlhu/MIRAGE>

a nearby reflective surface, as illustrated in Fig. 1. This may occur, for instance, when the sensors are placed on a table such as in voice-based assistant devices or next to a wall. The reflective surface is assumed to be the most reflective and closest one to the microphones in the environment, hence generating the strongest and earliest echo in each microphone. Under this *close-surface* model, we ask the following questions:

1. Can early echoes be estimated from two-microphone recordings of an unknown source?
2. Can they be used to estimate both the azimuth and elevation angles of the source, an *impossible* task in free field conditions?

We propose to use a deep neural network (DNN) trained on a simulated close-surface dataset to estimate early echoes properties from audio features. The MIRAGE framework then exploits these estimated properties by expressing them as TDOAs in the *virtual 4-microphone array* formed by the true microphone pair and its image with respect to the reflective surface. We show that the proposed framework approximately estimates echo properties, perform similarly to a correlation-based method in azimuth estimation for the considered scenario and estimates *impossible* elevation angles with good accuracy in noiseless settings using two microphones only.

2. BACKGROUND IN MICROPHONE ARRAY SSL

In this section, we briefly review some necessary background in microphone array SSL. Let us assume a microphone array of I sensors is placed inside a room and records the sound emitted by one static point sound source. In all generality, the relationship between the signal $m_i(t)$ recorded by the sensor placed at fixed position \mathbf{m}_i and the signal $s(t)$ emitted by the source at fixed position \mathbf{s} is defined by:

$$m_i(t) = (h_i * s)(t) + n_i(t), \quad (1)$$

where the convolution with room impulse response (RIR) $h_i(t)$ embodies the fact that sensor i receives a so-called spatial image of the source and n_i denotes possible measurement noise. The RIR depends on the spatial parameters of the scene: microphone positions, source position w.r.t the room, as well as the room acoustic properties (size, absorption and diffuseness of the wall materials.)

RIRs can be typically modelled as the sum of the direct path and multiple reflections of the sound. This can boil down to modelling h_i as a Dirac impulse at time τ_i accounting for the time delay from the source to microphone i , plus an error term. In the frequency domain, this leads to:

$$H_i(f) = \alpha_i(f) e^{-2\pi f \tau_i} + \varepsilon_i(f), \quad (2)$$

where the error term $\varepsilon_i(t)$ collects echoes, the reverberation tail, diffusion, and noise. The term $\alpha_i(f)$ captures the air attenuation phenomenon. A time-domain example of RIR is shown in Fig. 2 (left).

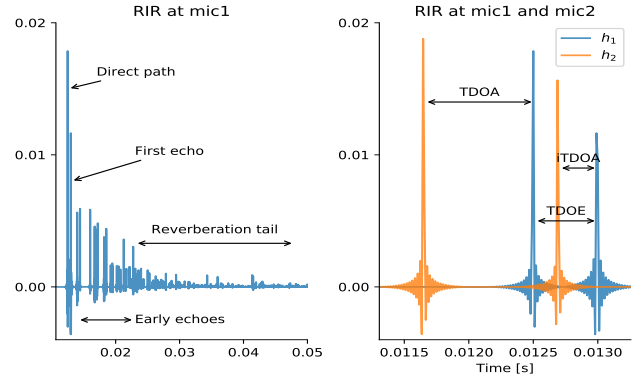


Fig. 2: Left, a typical simulated RIR with annotated components. Right, superposition of two RIRs and visualization of time difference of arrival between direct paths (TDOA), first echoes (iTDOA) and direct path and first echo (TDOE).

2.1. 2-channel 1D-SSL

Let us first consider the stereo case ($I = 2$). Under the far-field assumption, traditional SSL methods use the time difference of arrival (TDOA), $\tau \triangleq \tau_2 - \tau_1$, as a proxy for the estimation of the angle of arrival (AOA), since:

$$\text{AOA} = \arccos(c \tau / d), \quad (3)$$

where c is the speed of sound and d the inter-microphone distance. SSL then reduces to estimating the TDOA, which can be done by cross-correlation-based methods such as the widely used and well performing generalized cross-correlation with phase transform (GCC-PHAT) method [3, 18]. Given short-time Fourier transforms M_1 and M_2 of the two microphones signals, the GCC-PHAT *angular spectrum* is defined as:

$$\Psi_{\text{GCC}}(\tau) = \sum_{f,n} \frac{M_1(f,n)M_2^*(f,n)}{|M_1(f,n)M_2^*(f,n)|} e^{-2\pi f \tau}. \quad (4)$$

Then, the TDOA estimate is given by $\hat{\tau} = \arg \max_{\tau} \Psi_{\text{GCC}}(\tau)$. Note that Ψ_{GCC} can also be expressed directly as a function of the AOA using (3), hence the term *angular spectrum*.

2.2. Multichannel 2D-SSL

When more microphones are available and the array is not linear, 2D-SSL can be envisioned. A possible approach is to use 1D-SSL on all pairs and combine their results, a principle which was successfully applied in the steered response power with phase transform (SRP-PHAT) method [4]. SRP-PHAT exploits the geometry of the microphone array and the estimated TDOAs from microphone pairs to return the DOA. In a nutshell, this algorithm aims to estimate a global angular spectrum $\Psi_{\text{SRP}}(\theta, \phi)$ which will exhibit a local maximum in the direction of the active source. First, a global grid of possible DOAs is defined according to a desired resolution and

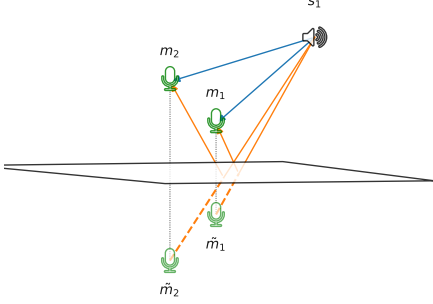


Fig. 3: Illustration of the images \tilde{m}_1 and \tilde{m}_2 of microphones m_1 and m_2 in the presence of a reflective surface and a source. Blue lines correspond to direct paths, orange lines correspond to echo paths.

computational load. Second, for each pair of microphones, a local set of AOAs is defined and a TDOA-based algorithm (e.g. GCC-PHAT) is used to compute the associated local angular spectrum. Finally all the local contributions (a collection of local $\Psi_{\text{GCC}}(\tau)$) are geometrical aggregated and interpolated back to the global DOA grid to form $\Psi_{\text{SRP}}(\theta, \phi)$, and the DOA maximizing Ψ is used as estimate.

3. MIRAGE: MICROPHONE ARRAY AUGMENTATION WITH ECHOES

We now introduce the proposed concept of microphone array augmentation with echoes (MIRAGE). Let us first expand formula (2) to account for more echoes:

$$H_i(f) = \sum_{k=0}^K \alpha_i^k(f) e^{-2\pi f \tau_i^k} + \varepsilon_i(f) \quad (5)$$

where the sum now comprises the direct path ($k = 0$) and the K earliest reflections ($K = 1$ in this paper) and ε_i collects the remaining RIR components. Here, $\alpha_i^k(f)$ accounts for both air attenuation and wall absorption phenomena. In the remainder of this paper, we make the approximation of frequency-independent α_i^k . Eq. 5 then corresponds to the well known image-source (IS) model, where reflections are treated as mirror images of the true source with respect to reflective surfaces, emitting the same signal. We will employ here a less common but equivalent interpretation of IS, namely, the image-microphone (IM) model. As illustrated in Fig. 3, virtual microphones are mirror images of the true microphones with respect to reflective surfaces. In this view, the echoic signal received at a true microphone is the sum of the anechoic signals received at this microphone and its images. If we consider the virtual array consisting of both true and image microphones, multiple microphone pairs are now available. For each of them, it is then possible to define a corresponding time difference of arrival. Among them, we will refer to the one between the two real microphones as TDOA, the one between the two image microphones as image TDOA (iTDOA)

and the one between the first microphone and its image as time difference of echoes (TDOE). We have:

$$\text{TDOA} = (\|\mathbf{m}_2 - \mathbf{s}\| - \|\mathbf{m}_1 - \mathbf{s}\|)/c = \tau_2^0 - \tau_1^0, \quad (6)$$

$$\text{iTDOA} = (\|\tilde{\mathbf{m}}_2 - \mathbf{s}\| - \|\tilde{\mathbf{m}}_1 - \mathbf{s}\|)/c = \tau_2^1 - \tau_1^1, \quad (7)$$

$$\text{TDOE} = (\|\tilde{\mathbf{m}}_1 - \mathbf{s}\| - \|\mathbf{m}_1 - \mathbf{s}\|)/c = \tau_1^1 - \tau_1^0, \quad (8)$$

where $\tilde{\mathbf{m}}_i$ denotes the image of position \mathbf{m}_i . These three quantities are directly connected to RIRs, as illustrated in Fig. 2(right). Let $V = \{\text{TDOA}, \text{iTDOA}, \text{TDOE}\} \in \mathbb{R}^3$. Following the 2D-SSL scheme described in Sec. 2.2 and given the virtual microphone-array geometry (which depends on the relative position of microphones to the surface), V could in principle be used to estimate the 2D directional of arrival of the source. In the next section, we present a learning-based method to estimate V using audio features obtained from only two microphones.

4. LEARNING-BASED ECHO ESTIMATION

Our approach is to train a deep neural network (DNN) on a dataset simulating the considered close-surface scenario. We model the problem as multi-target regression, with *interaural level difference* (ILD) and *interaural phase difference* (IPD) as input features, and $V \in \mathbb{R}^3$ as output parameters. ILD and IPD features are defined in the frequency domain as follows:

$$\begin{cases} \text{ILD}(f) = \frac{1}{T} \sum_{t=1}^T \log \left| \frac{M_2(f,t)}{M_1(f,t)} \right| \\ \text{IPD}(f) = \frac{1}{T} \sum_{t=1}^T \frac{M_2(f,t)/|M_2(f,t)|}{M_1(f,t)/|M_1(f,t)|} \end{cases} \quad (9)$$

More precisely, the input of the network is $\mathbf{x} = [\text{ILD}, \text{Re}(\text{IPD}), \text{Im}(\text{IPD})]$, where Re and Im denote real and imaginary part operators, respectively. Note that for the IPD, the frequency $f = 0$ is discarded because it is constant for every observation. In general, the mapping between V and the proposed feature is not unique. In particular, this happens when $\tau_2^1 = \tau_1^1$. In order to avoid this, we preventively pruned all the entries with $|\tau_2^1 - \tau_1^1| < 10^{-6}$ from the dataset.

We use a simple fully-connected DNN architecture consisting of a D -dimensional input layer, a 3-dimensional output layer, and 3 fully connected hidden layers with respective input sizes 500, 300 and 50. Rectified linear unit (ReLU) activation functions are used except at the output layer, and each hidden layer has a dropout probability $p_{\text{do}} = 0.3$. We use the mean square error loss function for training and the Adam optimizer [19]. The normalized root mean square error (nRMSE) is taken as validation metric¹. The network is manually tuned on a validation set to find the best combination of number of hidden layers, their sizes and p_{do} . Once time delay estimates \hat{V} are returned by the DNN, they are converted to synthetic local angular spectra and passed to Ψ_{SRP}

¹The nRMSE takes values between 0 (perfect fit) and ∞ (bad fit). If it is equal to 1, then the prediction is no better than a constant.

(See Sec. 2.2) together with the relative positions of true and image microphones which are assumed known. We call this algorithm MIRAGE. The synthetic local angular spectra consist of Gaussians centered at \hat{V} and with variances equal to the prediction errors made by the DNN on the validation set.

5. IMPLEMENTATION AND RESULTS

To the best of the authors’ knowledge, no reference implementation of algorithms for 2D-SSL using only 2 microphones is available to date. To check the validity of TDOA estimation, it is compared to GCC-PHAT using the true microphones (see Sec. 2.1). For training and validation of the DNN we generate many random shoe-box room configurations using the software presented in [20]. This software implements both the image-method for simulating reflections and a ray-tracing algorithm for diffusion. Room widths are uniformly drawn at random in [3, 9] m, heights in [2, 4] m. Random source/microphones positions and absorption coefficients for the 6 surfaces are used, respecting the close-surface scenario. In particular, the microphones are at most 30 cm from the close-surface, placed 10 cm from each other, the absorption coefficients of the other walls are uniformly sampled in (0.5, 1) and the one of the close-surface is in (0, 0.5). The same realistic diffusion profile [11] is used for all surfaces. Around 90,000 audio scenes are generated this way, yielding reverberation times (RT_{60}) between 20 ms and 250 ms. For training and validation, the RIRs are convolved with 1 sec of white-noise (wn) with no additional noise. All signals and RIRs are sampled at 16 kHz. The STFT is performed on 1024 point with 50% overlap. Finally the features are computed as in (9) yielding a vector of size $D = 1534$ for each observation. While we validate the DNN on a portion of the dataset in a *holdout* fashion, the test is conducted on 200 new RIRs convolved with both wn and speech (sp) utterances. This set is generated similarly to the training and validation sets. Moreover the recordings are perturbed by external white noise at 10 dB SNR (wn+n, sp+n). The speech signals are normalized speech utterances of various lengths (from 1 s to 6 s), randomly selected from the TIMIT corpus. A free and open-source Matlab implementation of SRP-PHAT² is used to aggregate local angular spectra obtained from the DNN’s output. A sphere sampling with 0.5° resolution and coordinates $\theta \in [-179, 180]$ and $\phi \in [0, 90]$ is used for the DOA search.

TDOA estimation errors using the proposed approach and GCC-PHAT are presented in Table 1. Training a DNN to estimate TDOAs brings similar performances as GCC-PHAT in terms of nRMSE. Estimation of iTDOA and TDOE seems to be a harder task for the simple DNN we used. Nevertheless, our results confirm the possibility of retrieving early echoes from only two-microphone recordings. When some external noise is added, performance of both methods severely

	Input	nRMSE			ACCURACY	
		TDOA	iTDOA	TDOE	$\theta < 10^\circ$	$\theta < 20^\circ$
MIRAGE	wn	0.18	0.28	0.25	4.10 (77)	5.97 (97)
MIRAGE	wn+n	0.68	0.69	0.89	5.00 (26)	9.89 (54)
MIRAGE	sp	0.31	0.34	0.56	4.83 (63)	7.26 (82)
MIRAGE	sp+n	0.99	0.98	1.48	4.60 (16)	9.88 (35)
GCC-PHAT	wn	0.21	-	-	4.22 (81)	6.19 (97)
GCC-PHAT	wn+n	0.68	-	-	4.03 (65)	5.34 (83)
GCC-PHAT	sp	0.32	-	-	4.08 (82)	5.34 (97)
GCC-PHAT	sp+n	1.38	-	-	4.70 (19)	8.38 (32)

Table 1: Normalize root mean squared error for TDOA estimation and mean angular error in $^\circ$ (with accuracies (%)) for AOA estimation with 10° and 20° angular tolerance.

DoA		ACCURACY < 10°		ACCURACY < 20°	
	Input	θ	ϕ	θ	ϕ
MIRAGE	wn	4.5 (59)	3.9 (71)	6.8 (79)	5.9 (88)
MIRAGE	wn+n	4.4 (18)	5.5 (26)	9.4 (35)	11.1 (66)
MIRAGE	sp	4.6 (45)	4.8 (59)	8.1 (71)	7.2 (83)
MIRAGE	sp+n	5.2 (17)	5.9 (12)	10.7 (38)	12.3 (43)

Table 2: Mean angular error in $^\circ$ (with accuracies (%)) for 2D SSL (azimuth and elevation) with 10° and 20° tolerance.

degrades. This is a well-know and expected behaviour for GCC-PHAT. It suggests that noise should be considered in the training phase of MIRAGE. When we compare the performance in terms of AOA, the two methods yield the same accuracy within a 20° threshold, as can be see in Table 1. When a smaller tolerance is considered, GCC-PHAT outdoes the proposed approach in accuracy, with comparable errors. Again, when adding noise, performance decreases. In Table 2 the performance of the full 2D-SSL pipeline is showed. Within a tolerance of 20° , the MIRAGE model allows estimation of both azimuth and elevation of the target source. However since in our data the 2 microphones were free to move, the inclinations of the true and image pairs are rarely flat. While this helps elevation estimation, it reduces the accuracy of predicting the right azimuth. While external noise is again decreasing the accuracy dramatically, it is interesting to notice that our DNN model trained and validated with white noise sources somewhat generalizes to speech sources.

6. CONCLUSION

In this paper we demonstrated how a simple echo model could allow 2D SSL with only two microphones, using simulated data. Future research will focus on extending this proof-of-concept to real data. The problem of echo-delay estimation proved to be very challenging, and extensions of the proposed learning scheme will be developed to obtain more reliable estimations of angular spectra. Extensions of the method to better handle various types of noise and emitted signals will also be sought. Finally, applications of the MIRAGE framework to larger microphone arrays, higher order echoes and a variety of tasks beyond SSL will be explored.

²http://bass-db.gforge.inria.fr/bss_locate/

7. REFERENCES

- [1] Caleb Rascon and Ivan Meza, “Localization of sound sources in robotics: A review,” *Robotics and Autonomous Systems*, vol. 96, pp. 184–210, 2017.
- [2] S. Argentieri, P. Danès, and P. Souères, “A survey on sound source localization in robotics: From binaural to array processing methods,” *Computer Speech & Language*, vol. 34, no. 1, pp. 87–112, nov 2015.
- [3] C. Knapp and G. Carter, “The generalized correlation method for estimation of time delay,” *IEEE Transactions on Acoustics, Speech, and Signal Processing*, vol. 24, no. 4, pp. 320–327, aug 1976.
- [4] Joseph H. DiBiase, Harvey F. Silverman, and Michael S. Brandstein, “Robust Localization in Reverberant Rooms,” in *Microphone Arrays: Signal Processing Techniques and Applications*, pp. 157–180. Springer, Berlin, Heidelberg, 2001.
- [5] Romain Lebarbenchon, Ewen Camberlein, Diego Carlo, Antoine Deleforge, and Nancy Bertin, “Evaluation of an open-source implementation of the SRP-PHAT algorithm within the 2018 LOCATA challenge,” in *2018 IEEE-AASP Challenge on Acoustic Source Localization and Tracking (LOCATA), International Workshop on Acoustic Signal Enhancement*, 2018, pp. 2–3.
- [6] Jan Scheuing and Bin Yang, “Disambiguation of tdoa estimates in multi-path multi-source environments (datemm),” in *ICASSP (4)*, 2006, pp. 837–840.
- [7] Antoine Deleforge, Florence Forbes, and Radu Horaud, “Acoustic space learning for sound-source separation and localization on binaural manifolds,” *International Journal of Neural Systems*, vol. 25, no. 01, pp. 1440003, 2015.
- [8] Fabio Vesperini, Paolo Vecchiotti, Emanuele Principi, Stefano Squartini, and Francesco Piazza, “A neural network based algorithm for speaker localization in a multi-room environment,” in *2016 IEEE 26th International Workshop on Machine Learning for Signal Processing (MLSP)*. Sep. 2016, pp. 1–6, IEEE.
- [9] Sharath Adavanne, Archontis Politis, and Tuomas Virtanen, “Direction of arrival estimation for multiple sound sources using convolutional recurrent neural network,” *CoRR*, vol. abs/1710.10059, 2017.
- [10] Lauréline Perotin, Romain Serizel, Emmanuel Vincent, and Alexandre Guérin, “CRNN-based multiple DoA estimation using Ambisonics acoustic intensity features,” *IEEE Journal of Selected Topics in Signal Processing (submitted)*, 2018.
- [11] Clément Gaultier, Saurabh Kataria, and Antoine Deleforge, “VAST : The Virtual Acoustic Space Traveler Dataset,” in *International Conference on Latent Variable Analysis and Signal Separation (LVA/ICA)*, Grenoble, France, Feb. 2017.
- [12] Hiromichi Nakashima, Mitsuru Kawamoto, and Toshiharu Mukai, “A localization method for multiple sound sources by using coherence function,” *European Signal Processing Conference*, vol. 1, no. 3, pp. 130–134, 2010.
- [13] Ivan Dokmanić, Reza Parhizkar, Andreas Walther, Yue M Lu, and Martin Vetterli, “Acoustic echoes reveal room shape,” *Proceedings of the National Academy of Sciences*, vol. 110, no. 30, pp. 12186–12191, 2013.
- [14] Inkyu An, Myungbae Son, Dinesh Manocha, and Sung-Eui Yoon, “Reflection-Aware Sound Source Localization,” in *2018 IEEE International Conference on Robotics and Automation (ICRA)*. may 2018, pp. 66–73, IEEE.
- [15] James L Flanagan, Arun C Surendran, and Ea-Ee Jan, “Spatially selective sound capture for speech and audio processing,” *Speech Communication*, vol. 13, no. 1-2, pp. 207–222, 1993.
- [16] Ivan Dokmanić, Robin Scheibler, and Martin Vetterli, “Raking the cocktail party,” *IEEE journal of selected topics in signal processing*, vol. 9, no. 5, pp. 825–836, 2015.
- [17] Robin Scheibler, Diego Di Carlo, Antoine Deleforge, and Ivan Dokmanic, “Separake: Source separation with a little help from echoes,” in *2018 IEEE International Conference on Acoustics, Speech and Signal Processing, ICASSP 2018, Calgary, Canada, Apr. 15-20, 2018*, pp. 6897–6901.
- [18] Charles Blandin, Alexey Ozerov, and Emmanuel Vincent, “Multi-source TDOA estimation in reverberant audio using angular spectra and clustering,” *Signal Processing*, vol. 92, no. 8, pp. 1950–1960, 2012.
- [19] Diederik P. Kingma and Jimmy Ba, “Adam: A method for stochastic optimization,” *CoRR*, vol. abs/1412.6980, 2014.
- [20] Steven M Schimmel, Martin F Muller, and Norbert Dillier, “A fast and accurate shoebox room acoustics simulator,” in *IEEE International Conference on Acoustics, Speech and Signal Processing, ICASSP 2009, 2009*, pp. 241–244.